

Effect of the momentum transfer on the Rayleigh scattering cross section

M. Skowronek and Y. Alayli*

*Laboratoire de Physique et Optique Corpusculaires (Plasmas denses), Université Pierre et Marie Curie, Tour 12-E5,
4 Place Jussieu, 75230 Paris, Cedex 05, France*

(Received 16 June 1978)

The Rayleigh scattering cross section is measured with a short-duration pulse of laser light in different gases. It depends on the pulse duration, involving a time constant τ , following the expression $S_{\text{exp}}/S_{\text{theor}} = (\tau_1/\tau) (1 - e^{-\Delta t/\tau})$, where S_{exp} and S_{theor} are the experimental and the theoretical cross sections and τ_1 is the classical time constant corresponding to the dipole damping. The time constant τ was determined with a ruby laser whose pulse half-width was varied between 6 and 200 nsec. Using a tunable dye laser and its nitrogen laser pump, the authors have found that τ is proportional to λ^2 (square of the wavelength). The variation of τ for gases of different molecular sizes shows that τ is proportional to their diameter a . The angular distribution of the scattered light has been determined and found to be favored in the forward direction. The constant τ is proportional to $\sin(\theta/2)$ (where θ is the scattering angle), i.e., to the momentum transfer. By analogy with a corpuscular collision, dimensional considerations lead to the formula $\tau = 0.85(\lambda/\lambda_c)^2(a/c)\sin(\theta/2)$ (λ_c is the Compton wavelength), which well describes the experimental results.

I. INTRODUCTION

The molecular scattering of light by gases has been widely studied and is currently considered to be thoroughly understood. As early as 1929, Cabannes¹ reviewed the main experimental results obtained by means of conventional light sources. These measurements were apparently a complete confirmation of the Rayleigh theory. The laser, which is very efficient tool for investigating the thermodynamics of fluids, particularly for the study of the scattered light spectrum,^{2,3} has brought about a resurgence of interest in this field. The beautiful results obtained in this field of physics have led numerous physicists to apply this technique to the diagnostics of plasmas. A common method used to calibrate a Thomson scattering device consists in replacing the plasma by a gas and measuring the Rayleigh scattering. The present work has been undertaken with a view toward calibrating the scattering device using short-duration laser pulses. We have observed systematic discrepancies with the theoretical predictions in spite of increased efforts for improving the accuracy of all the elements entering the determination of the scattering cross section. This has led us to analyze in a detailed way the available literature on absolute Rayleigh scattering cross sections.

We present, first, a historical survey which justifies our basic motivation. After that, a brief summary of the classical Rayleigh theory is given, in order to introduce the notations. We describe then the experimental device and the results obtained with random pulse duration. Rayleigh scattering cross sections are then given as a function

of pulse duration, laser wavelength, molecular diameter, and scattering angle. The results are presented through a time constant characterizing the process.

From the analogy with corpuscular collisions and from the use of the uncertainty principle, we have built an analytical compact expression which describes satisfactorily all our results and gives insight to the microscopic mechanism involved.

II. HISTORICAL BACKGROUND

Although general agreement with Rayleigh's theory was claimed, Cabannes¹ and Daure⁴ found that the absolute values of the scattering cross sections were about 20% smaller than the theoretical ones. This was later confirmed by different authors who measured the atmospheric transparency. Although some controversy exists between them, Dufay⁵ and Duclaux⁶ agree on one point; the experimental scattering cross sections seem to be (20–25)% smaller than the theoretical ones.

De Vaucouleurs⁷ measured the Rayleigh ratio in air and argon. He claimed that the precision of his measurements was better than 0.3%. But he determined the Avogadro number with a great dispersion. For instance, his extreme values were 4.173×10^{23} and 6.063×10^{23} . He gave no explanation for his choice, which corresponded to the best value available in the literature at the time, and was obtained by other methods.

The first measurement of the differential cross section at an angle of 90° by means of a cw He-Ne laser was made by Geindre *et al.*⁸ Using photon-counting techniques, they found the theoretical value. But since their value was given within 20% error, we will see that our experimental

value at 90° for long-pulse duration is in this range.

Other measurements performed with a ruby laser indicate a discrepancy with the theory. George *et al.*,⁹ using the pulses of the relaxation regime (having a long duration), measured the differential scattering cross section at an angle of 60° . They found a value about two times greater than the theoretical one and an angular distribution in discrepancy with Rayleigh's theory. In fact, the Rayleigh angular distribution is uniform. The laser was focused into the scattering chamber and this complicated the determination of the scattering volume. The level of parasitic light was rather high, about twice the scattered light at 1 atm.

Watson and Clark¹⁰ measured the angular distribution. They did not find any departure from the theory, but it is not clear whether they took into account the variation of the scattering volume with the angle.

Rudder and Bach¹¹ also measured the scattering cross section at 60° for N_2 ; their results agreed with the theoretical value. A calculation based on geometrical optics was employed to find the scattering volume viewed by the detection optics. This may be the origin of substantial errors because the scattering volume is limited by lines originating on diaphragm edges far from this volume.

Some theoretical works¹²⁻¹⁵ have tried to explain the results obtained by George *et al.*⁹ For instance, Gabriel¹⁵ criticized the Rayleigh theory, viz., since the random motion of the molecules affects the phase of oscillations, the validity of the various Fourier transforms is doubtful. Gabriel attempted to build a self-consistent explicit microscopic theory. He obtained a good interpretation of the spectrum of the scattered light and found an additional term in the integrated intensity which affected the angular distribution. But, like the others, he was not able to explain the results of George *et al.*⁹

Thus it is necessary to clear up the experimental situation in order to provide a firm basis for a microscopic theory and a transient analysis, and to obtain a sound calibration of the optical system that measures the Thomson scattering. It should be noted that some plasma diagnostics based on light scattering has given anomalous results which have not yet been confirmed by other methods.¹⁶⁻¹⁹

III. REVIEW OF THE MAIN FEATURES OF THE RAYLEIGH THEORY

The geometry of the scattering experiment is chosen as follows: the incident light propagates

along the z axis and is polarized along the x axis. The scattered light is observed in a direction D at an angle θ in the plane yz . The equation of motion of the electron is

$$\ddot{x} + \omega_0^2 x + \gamma \dot{x} = (e/m)E, \quad (1)$$

where ω_0 is the fundamental frequency of the dipole, E is the incident electric field at frequency ω , and γ is the damping due to the emitted light:

$$\gamma = (1/6\pi\epsilon_0)(e^2\omega^2/mc^3).$$

The polarizability is defined by $\alpha = ex/\epsilon_0 E$ and it is found that

$$\alpha^2 = \frac{e^4}{m^2\epsilon_0^2} \frac{1}{(\omega_0^2 - \omega^2)^2 + \gamma^2\omega^2}.$$

The scattering cross section per atom is defined by

$$S = \frac{1}{n} \frac{P_d/\Omega}{P_0/s},$$

where P_d/Ω is the scattering power per unit solid angle, P_0/s is the incident power per unit surface, and n is the molecular number density. It is easy to show that $S = \pi^2\alpha^2/\lambda^4$. The textbooks currently emphasize the fundamental distinction between the scattering and the fluorescence process. The first mechanism is not considered as an absorption in opposition to the second.

However, two remarks should be made: (i) the scattering mechanism involves some intermediate states in a complex scheme, and (ii) the equation would not differ if the process was considered as an absorption.

If we calculate an absorption coefficient based on Eq. (1), the light scattered in all directions corresponds exactly to the light eventually absorbed by the damping mechanism. S may be written as $S \sim \gamma\omega^2\alpha^2$ or

$$S \sim A/\tau_1, \quad (2)$$

where τ_1 is the time constant associated with the damping $\tau_1 = 1/\gamma$. Since the value of τ_1 is 22 nsec at $\lambda = 694.3$ nm, a question is raised about the behavior of the scattering with short pulse duration.

IV. EXPERIMENTAL SETUP AND PRELIMINARY MEASUREMENTS (REF. 20)

The experimental setup (see Fig. 1) was designed for measuring precisely all the geometrical parameters: the scattering volume, the angle of scattering, the solid angle of observation, and the polarization of the light. We were able to reduce to a low level the spurious diffracted light and thus, we obtained reliable data on the scattering intensity. This scattered light is brought, for each gas, to a sufficient level by increasing the density

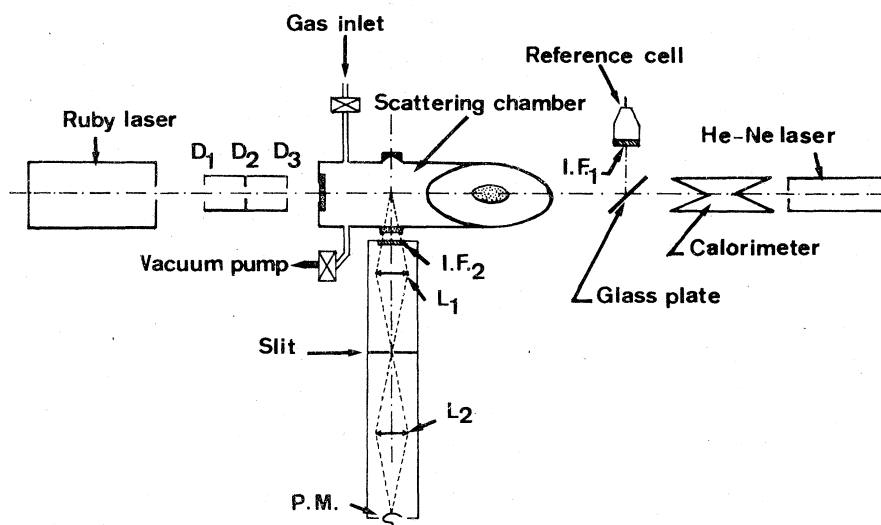


FIG. 1. Experimental setup. D_1 , D_2 , and D_3 are the diaphragms; IF, and IF₂ are the interference filters; L_1 and L_2 are the lenses of the detection device; P. M. is the measuring photomultiplier; the ruby-laser polarization is perpendicular to the plane of the figure; the exit glass plate is at Brewster angle. The He-Ne laser is used for aligning when the calorimeter is taken away.

in order to avoid the dispersion of the signals due to a transit-time dispersion which becomes important for short-duration pulses and due to the random character of the electronic multiplication. Since the mean number $\langle N \rangle$ of photoelectrons equals $\langle \Delta N^2 \rangle$, the dispersion defined by $\langle \Delta N^2 \rangle^{1/2}$ is proportional to $\langle N \rangle^{-1/2}$ and decreases at a high-intensity light level. Pressures up to 15 atm may be reached. On the other hand, we have carefully avoided the saturation effects arising on the photocathode and on the dynodes.

The beam is not focused. The intensity of the laser is then insufficient to produce nonlinear effects or ionization. This also makes the scattering volume very nearly a cylinder. Three diaphragms D_1 , D_2 , and D_3 are placed in the light path to confine the beam diameter to a precise value. The scattering chamber is blackened and also contains some light baffles. The exit window is at the Brewster angle for minimizing the spurious reflection of the laser beam. Research grade gases are used and a cotton filter guards against dust in the chamber. The chamber is evacuated from time to time in order to clean it.

A glass plate reflects a part of the emerging beam which is conveniently attenuated, onto a photodiode (Radiotechnique XA 1003) having a rise time of 0.2 nsec. This cell is used for normalization. It also records the real shape of the incident pulse. After leaving the chamber, the laser beam is absorbed on the graphite cone of a calorimeter.

The scattered light crosses a clean optical window and enters the detection system through an interference filter centered at 694.3 nm (in the case of the ruby laser). The scattering volume is first imaged on a variable slit. The image of the slit is projected on the measuring photomultiplier with a geometric magnification ratio of 1. Two different

photomultipliers were used depending on the pulse duration. The first one (Radiotechnique 56 T.V.P) has a 2 nsec rise time and 10^8 amplification; the second one (Radiotechnique XP 2020) has a 0.9-nsec rise time and 10^7 amplification. At each shot, the reference and scattered pulses are displayed on an oscilloscope (Tektronix 7904) having a rise time of 0.2 nsec.

The following preliminary checks were made prior to each new set of measurements.

(a) A determination of the incident light polarization vector.

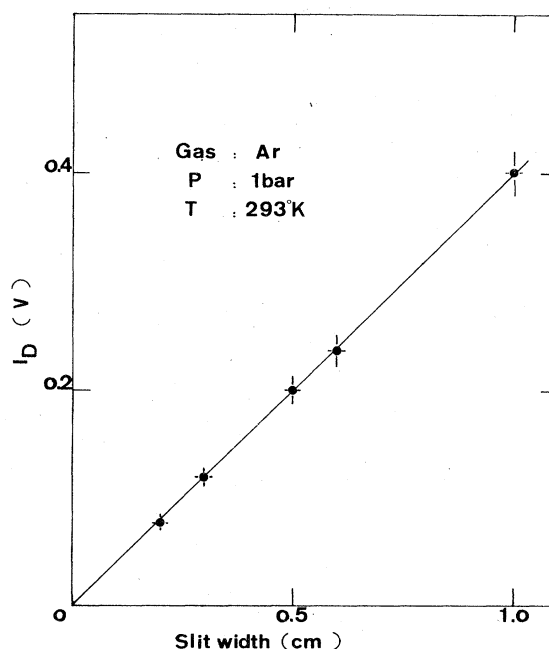


FIG. 2. Variation of light registered on the photomultiplier I_D vs the slit width. The scattering volume is replaced by an auxiliary source.

(b) A measurement of the scattering volume; the diameter of the laser beam is carefully measured at the place of the scattering owing to a slight divergence. The length is defined by the slit of the detection device and is controlled by means of an auxiliary homogeneous source (see Fig. 2). For the angular distribution study another scattering chamber allowing measurements at $\theta = 30^\circ$, 45° , 60° , 90° , 120° , and 135° was used. In this case, the scattering volume is seen through a constant slit 5 mm large. We have verified that this volume is proportional to $1/\sin\theta$ by means of an auxiliary homogeneous source replacing the scattering volume.

(c) A determination of the solid angle of observation: it is defined by the aperture of the first lens of the detection device. The linearity between the scattered intensity and the solid angle was verified for four values of the solid angle (see Fig. 3).

(d) A determination of the laser pulse shape: the ideal shape is that of a simple geometric form (triangle, Lorentzian, etc.) for which the half-width is well-defined. If the pulse has a very large base, as is sometimes the case, it is useful to consider it as the sum of two pulses of different duration.

(e) A determination of the scattered light at 1 atm: the variation of the scattered light versus the pressure is studied. This variation must be linear with the molecular density. This is verified. When it is necessary, a correction is applied which takes into account the equation of state of the gas. This illustrates the good precision of our measurements. We give as an example the determination of the scattered light at 1 atm for SF_6 (see the Appendix). The experimental curves versus pressure are fitted using the least-squares method; the uncertainty on the slope is less than 2%.

All these preliminary measurements are quite necessary. If they are not explicitly noted, the validity of the measurements can be suspected. This is the case for Refs. 9-11 and this may explain some negative results recently published.^{21,22}

V. MEASUREMENT OF THE RAYLEIGH SCATTERING CROSS SECTION AT RIGHT ANGLE BY MEANS OF A Q-SWITCH RUBY LASER

$\lambda = 694.3$ nm, $\theta = 90^\circ$, the gas is argon, and $\Delta t \approx 22.5$ nsec. Starting from the definition of the Rayleigh cross section

$$S = \frac{1}{N} \frac{P_d/\Omega}{P_0/s}$$

$N = nV$ is the total number of scatterers (n is the density and V the volume), P_d is the scattered power, Ω is the solid angle, P_0 is the incident

power, s is the area of the beam. Since $V = sL$, we may write

$$S = \frac{1}{nL} \frac{P_d/\Omega}{P_0}$$

Two methods are used to obtain P_d/P_0 :

(a) P_0 is measured by means of a calorimeter and P_d is determined by calibrating the optical detection device in reference to a tungsten ribbon lamp. This method is the more imprecise, due to the calorimeter, which is given for 20% precision.

(b) P_d/P_0 is measured directly by means of a pile of neutral filters. Each filter is carefully calibrated with a spectrophotometer. The additivity of these attenuators is controlled by combining them. The whole attenuation obtained is 4.8×10^{-11} . The precision is about 5%.

These two methods give results in agreement within 20% of each other. The result we have found is $S_{\text{expt}}/S_{\text{theor}} \approx 0.5$. We have observed that the results were much more dispersed than was possible from the experimental errors of the second method. This dispersion was correlated with a dispersion of the half-width.

We have observed that the longer the pulse, the larger the scattered intensity. We are led to class the pulses as a function of their duration. The dispersion is then greatly reduced and we find for the ratio of the experimental cross section over the theoretical one the following value:

$$S_{\text{expt}}/S_{\text{theor}} = 0.45 \pm 0.02 \text{ for } \Delta t = 22.5 \text{ nsec.}$$

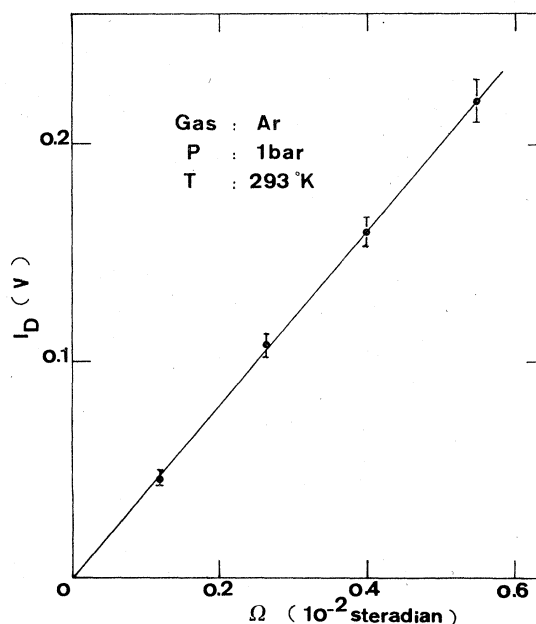


FIG. 3. Variation of the light measured on the photomultiplier I_D (S) with the solid angle of observation Ω in steradian.

As this ratio is related to the pulse half-width, we are interested in studying its variation with pulses of different duration.

VI. VARIATION OF THE RAYLEIGH SCATTERING CROSS SECTION WITH THE PULSE DURATION

$\lambda = 694.3$ nm, the gas is Argon, and $\theta = 90^\circ$. The ruby laser pulse duration is varied using the following methods.

(a) The laser works in a relaxation mode. The duration of the pulses varies from 100 to 200 nsec, the most probable value being 150 nsec. The power is 1 kW, at the maximum.

(b) In the Q-switch mode with a saturable dye glass in the cavity, the laser delivers pulses from 20 to 30 nsec. The power is about 20 MW.

(c) A diaphragm in the cavity shortens the pulse duration in the range 22–11 nsec. The power is about 1 MW. The spectral composition of the light is indeed not altered by the slight mode selection produced by the diaphragm.

(d) The laser light crosses a Pockels cell shutter. Pulses between 9–6 nsec are obtained. The shape of the pulses in this case, is not very regular. We must take into account a large base.

For all this duration range (6–150 nsec), we have observed that the scattered intensity is proportional to $1 - e^{-\Delta t/\tau}$, where Δt is the width of the pulse and τ is the time constant. Following Eq. (2) and because $\tau \neq \tau_1$, we must write for the ratio of the experimental cross section S_{expt} to the theoretical one S_{theor} .

$$\frac{S_{\text{expt}}}{S_{\text{theor}}} = (\tau_1/\tau)(1 - e^{-\Delta t/\tau}). \quad (3)$$

In Fig. 4, the experimental results are displayed; they follow relation (3). This formula is given for argon at right angle, with the wavelength $\lambda = 694.3$ nm, and the value $\tau = 28$ nsec. This time constant must be understood as connected to an emission probability. Indeed, the shape of the scattered pulse remains practically the same as that of the incident pulse. Moreover, no delay, greater than 2 or 3 nsec, between the incident and the scattered light, has been observed.

From now on, we will represent all experimental results, relative to the classical theoretical values, by the time constant τ as calculated by formula (3). Some of these measurements were already reported in Refs. 23 and 24.

VII. VARIATION OF THE TIME CONSTANT τ WITH WAVELENGTH

$\theta = 90^\circ$, the gas is argon, $\lambda = 337.1$ nm with $\Delta t \approx 4$ nsec, $\lambda = 651.7$ nm, 594.2 nm, and 481.5 nm with $\Delta t \approx 2$ nsec. In this study, we use a tunable dye laser pumped by a nitrogen laser. The light emission of the laser is carefully studied in order to obtain a regular pulse shape and an emission spot as homogeneous as possible. The fluorescent light emitted is amplified along the cavity axis at the same time as the laser emission, but at a slightly different wavelength. Then the fluorescent light constitutes a spurious emission which

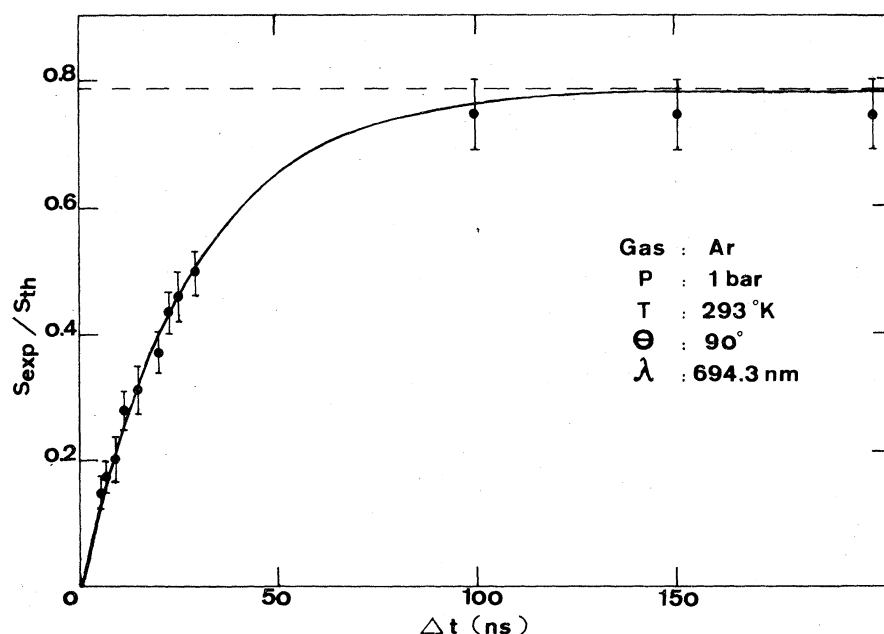


FIG. 4. Ratio of the Rayleigh scattering cross section measured S_{expt} on the theoretical value S_{theor} vs the pulse duration Δt (displayed in nanoseconds). The full line represents the curve $(1 - e^{-\Delta t/\tau})\tau_1/\tau$. Here $\tau_1 = 22$ nsec; $\tau = 28$ nsec; the broken line represents the asymptotic value τ_1/τ .

we have to minimize. Two tricks are used:

(a) A 1-mm diam diaphragm is put at the cavity exit for a spatial filtering. The dye cell is oriented to favor off-axis super-radiance.

(b) Since the super-radiant emission is more divergent than the laser one, the scattering chamber is placed far from the laser, and we put some diaphragms and a beam expander in the light path in order to ensure a low level of spurious light (always lower than 5%).

As the laser emission is not very powerful, we have used only three dyes at their optimum wavelength. It was not possible to use the wavelength variation given by a variable grating monochromator placed in the cavity. The characteristics of the light pulses are displayed in Table I.

The study of the statistics of the pulses has shown us that they follow a Poisson distribution. Again, naturally, for each wavelength the linearity of the scattered light with the density was checked. The intensity of the scattered light at 1 atm is determined by the least-squares method and the corresponding regression coefficient r^2 is given in the last column of Table I.

We have calculated the values of τ in each case. These values are displayed on Fig. 5. τ is found to be proportional to λ^2 as is the case for τ_1 . In the case when $\Delta t \gg \tau$ it can be seen that S_{expt} (as S_{theor}) is proportional to λ^{-4} . The curve is also consistent with the value obtained at $\lambda = 694.3$ nm with a much longer pulse.

VIII. VARIATION OF THE RAYLEIGH SCATTERING CROSS SECTION WITH THE NATURE OF THE GAS

$\theta = 90^\circ$; $\lambda = 694.3, 651.7, 594.8, 481.5,$ and 337.1 nm. For all the gases, the results are obtained relative to argon. The depolarization factor is

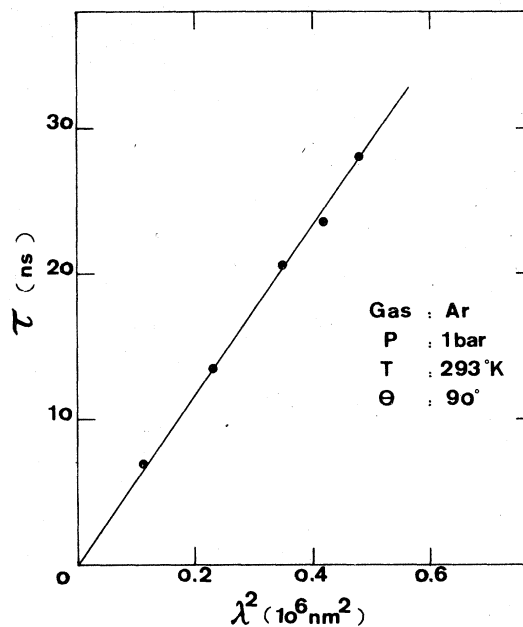


FIG. 5. Time constant τ (in nanoseconds) in function of the square of the wavelength λ^2 in 10^6 nm^2 .

taken into account in the case of molecules where this phenomenon occurs. The depolarization factors are given by Bridge and Buckingham.²⁵ For each gas, a value of the time constant τ was calculated in the same way as for argon.

For a great number of gases having a spherical structure, τ is found to be proportional to the molecular diameter. The experimental results are displayed in Fig. 6, where we have chosen a consistent set of values for the molecular diameters (here Lennard-Jones).

This proportionality ($\tau \sim a$) accounts for a slight

TABLE I. Characteristic values of the light pulses.

Dye	Wavelength (nm)	Approximate peak power	Approximate half-width	Coefficient of regression: r^2
Cresyl-violet	651.7	20 kW	3 nsec	0.992
Rhodamine 6G	594.2	50 kW	2.5 nsec	0.990
Umbelliferum U47	481.5	50 kW	1.9 nsec	0.991
Pump nitrogen laser	337.1	400 kW	4 nsec	0.999

TABLE II. Values of τ for a series of gases; comparison with the molecular diameter a .

Gas	a (Å)	Time constant τ (nsec)				
Ne	2.8	22.6
H ₂	2.9	23.5	19.5	16	11	...
Ar	3.45	28	23.5	20.4	13.5	7
Kr	3.6	28.6	24	20.2	13	...
O ₂	3.45	27.2	22	19	13	...
N ₂	3.7	28.4	23.6	20.4	14	...
CO	3.6	30	24.4	20.6	14	...
NO	3.55	28.2
N ₂ O	3.85	28.8
CO ₂	3.95	30.1	25.8	21.8	15.8	...
SF ₆	5	36	31	26	19	...
CH ₄	3.8	27.6	24	21.2	15.6	...
C ₂ H ₆	4.4	28
C ₂ H ₄	4.22	27.3	25.2	21	16.4	...
C ₂ H ₂	4.22	30.3
λ (nm)	694.3	651.7	594.2	481.5	337.1	

difference with the theory, which is observed, when we compare two gases. This is valid for Ne, Kr, H₂, O₂, N₂, CO, CO₂, NO, N₂O, CH₄, and SF₆. For more complex hydrocarbon molecules, like C₂H₆, C₂H₄, or C₂H₂, this proportionality is no longer observed. The effective diameter rather refers to a portion of the molecule, for instance, the chain C-H (see Table II). But more work is necessary to determine the effect of the molecular structure (apart from the well-known effect coming from the polarizability) on the Rayleigh scattering.

IX. ANGULAR DISTRIBUTION OF THE SCATTERED LIGHT

$\lambda = 694.3$ nm, $\Delta t \approx 30$ nsec, and the gas is argon. The Rayleigh scattering is measured in each direction, relative to the scattered intensity at right angle. It is normalized to a constant scattering volume. The angular distribution of the scattered light from the ruby laser beam lasting about 30 nsec in argon is shown in Fig. 7. The scattering is strongly favored in the forward directions. It is possible to calculate the value of the time constant τ in each direction, using formula (3). The results are displayed in Fig. 8. We have observed that τ is proportional to $\sin^{\frac{1}{2}}\theta$. This may be interpreted by saying that τ is proportional to the momentum variation which is undergone by the photon in the scattering process.

It is possible to recalculate what angular distribution we would obtain with a pulse having a duration $\Delta t \gg \tau$. This is displayed in Fig. 9. This distribution is compared with the results of George *et al.*,⁹ which are corrected with the proper scat-

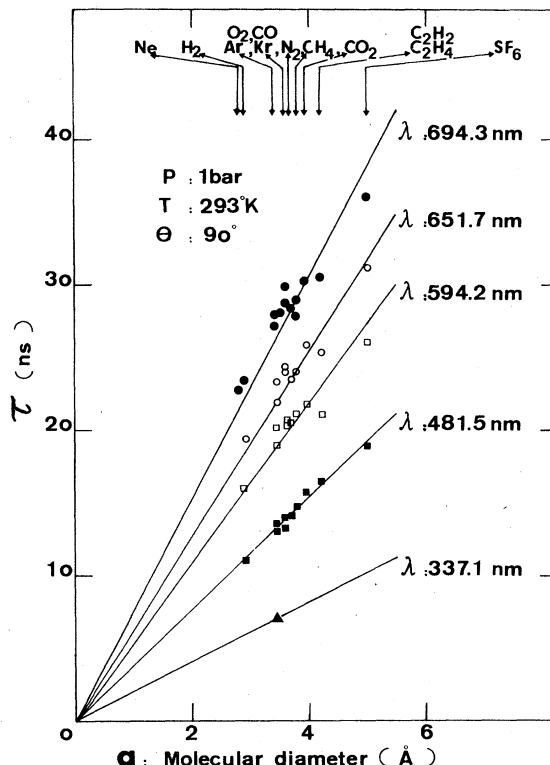


FIG. 6. Time constant τ (in nanoseconds) versus the molecular diameter a (in angstroms). The names of the different gases are given in the upper part. The wavelength λ is taken as a parameter.

tering volume variation. Now it can be seen that the experimental angular distribution of Ref. 9 is in reasonable agreement with our calculation. There is no contradiction with their absolute measurement at 60° giving a value two times the theoretical one, performed with a long pulse, and our measurement at 90° giving a value about one-half the theoretical one, with a short pulse.

We also reconfirm that the scattered-light angular distribution does not correspond to the forecast of Rayleigh's theory, which states a uniform distribution.

X. DISCUSSION

We have measured the absolute Rayleigh cross section taking great care concerning the geometric factors and the shape and homogeneity of the laser beam. About 10^4 experiments were made.

We have established that the Rayleigh scattering cross section depends on a time constant following (3):

$$S_{\text{expt}}/S_{\text{theor}} = (\tau_1/\tau)(1 - e^{-\Delta t/\tau}).$$

For short pulses of light, ignoring this time dependence may introduce large errors if the Ray-

leigh scattering is used to calibrate a Thomson scattering device for diagnostic purposes. Moreover we have found that, even when $\Delta t \gg \tau$ (infinite), the scattering cross section in oxygen and nitrogen is about 20% lower than the theoretical one and we are able to reconfirm very old measurements.⁴⁻⁶

We have shown that the angular distributions of the scattered light is favored in the forward directions. We agree then with the results obtained by George *et al.*,⁹ about 15 years ago, with one of the first ruby lasers.

The time constant τ , as calculated by formula (3) is proportional to the square of the wavelength λ , to the molecular diameter a , and to $\sin^2 \theta$, where θ is the scattering angle:

$$\tau \sim \lambda^2 a \sin^2 \theta.$$

This time constant is independent of the molecular density in all our experiments. The scattered intensity varies linearly with the incident intensity in the range 40 kW–20 MW and with the molecular density, from 0.1 to 15 atm.

These results suggest that τ takes its origin

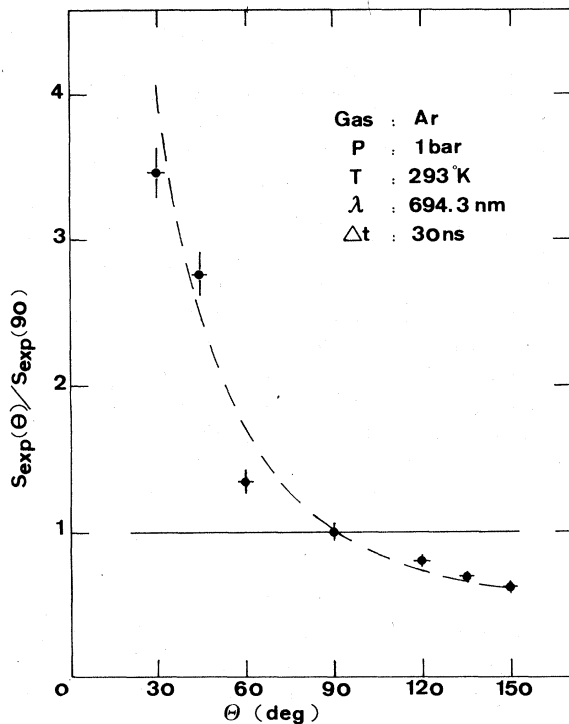


FIG. 7. Relative angular distribution of the scattered light intensity. Ratio of the measured value at an angle θ ; $S_{\text{exp}}(\theta)$ over the measured value at $90^\circ = S_{\text{exp}}(90^\circ)$. This ratio is given vs the scattering angle θ (in degrees). The full line is Rayleigh's theory; the broken line is the calculation based on formula (8), $\tau(\theta) = \tau(90^\circ) 2 \sin^2 \theta / \sqrt{2}$. The dots are the experimental values.

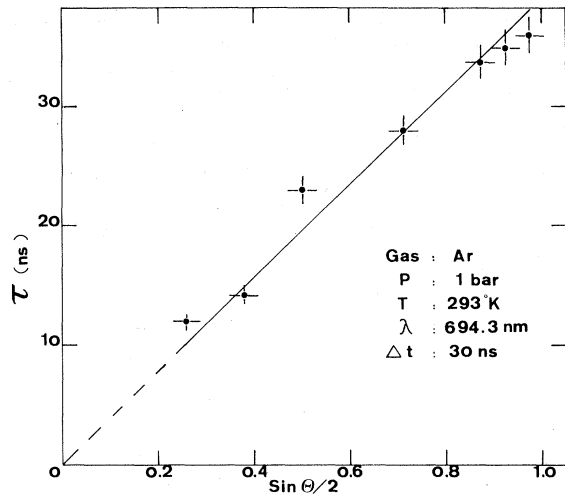


FIG. 8. Time constant $\tau(\theta)$ (in nanoseconds) vs $\sin^2 \theta$. τ is calculated by the formula (3); $S_{\text{exp}}/S_{\text{theor}} = (1 - e^{-\Delta t/\tau}) \tau_1/\tau$.

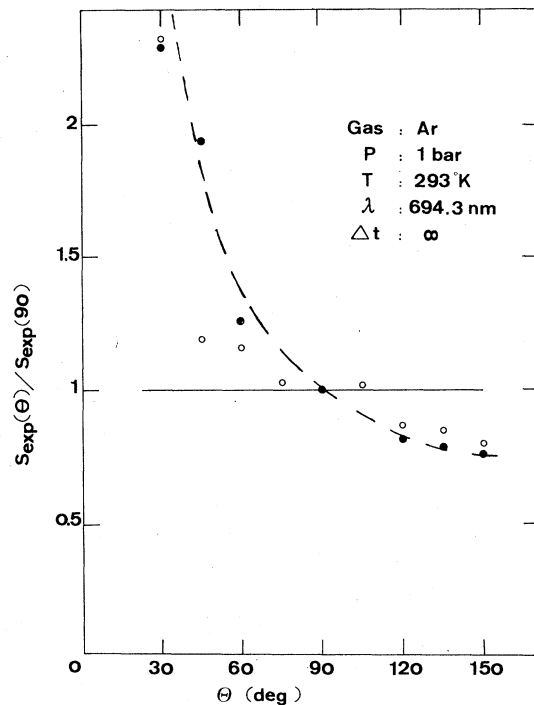


FIG. 9. Angular distribution of the scattered intensity, calculated in the case of very long pulse ($\Delta t \gg \tau$) in argon at $\lambda = 694.3$ nm. Black dots are extrapolation from our experimental points obtained with 30-nsec pulses. White dots are experimental points of Ref. 9 corrected with the proper scattering volume variation. Full line is Rayleigh's theory. Broken line is $\sqrt{2}/2 \sin^2 \theta$.

from the momentum exchange and that one must carefully reexamine the microscopic collision describing the reaction:

(incoming photon) + atom \rightarrow (outgoing photon) + atom.

Indeed, the experiments we have described above are analogous to collision experiments where electrons are directed toward atomic targets for studying the electron-atom potential. Sometimes it happens that the colliding particle is captured during a short time. Similarly, we may use the same language, knowing that the wavelength associated with the particle is, in our case, the wavelength of the light.

If we assume that the basic mechanism is that of a three-body collision, we can show that the time constant τ comes from the uncertainty relation. Prigogine²⁶ states that, in a three-body collision, an intermediate state is formed. This state has a lifetime proportional to a/k^2 , where a is the molecular diameter and k is an average momentum. Moreover, it is known that, when a perturbation is suddenly applied to an atomic system, this time is proportional to the perturbation $\tau \sim \Delta k/k$. So our τ is proportional to

$$(a/k^2)(\Delta k/k) \sim a\lambda^2 \sin^{\frac{1}{2}}\theta. \quad (4)$$

Thus we recover the main features of the variation of τ . A value for the proportionality coefficient can be determined as follows, with the uncertainty relation $\tau \approx h/\Delta E$; we may write $\Delta E \approx \hbar^2 k^2/2m$ and we find that τ is proportional to $2\lambda^2 m/h$. If we compare with formula (4), we can write

$$\tau = 2\lambda^2(m/h)(a/L) \sin^{\frac{1}{2}}\theta,$$

where L is a length to be determined. If we take m as the electron mass and if we introduce the Compton wavelength $\lambda_c = h/mc$

$$\tau = 2(\lambda^2/\lambda_c)(a/cL) \sin^{\frac{1}{2}}\theta. \quad (5)$$

If we compare (5) with the experimental results we find $L \approx \lambda_c$, and finally

$$\tau = 0.85(\lambda/\lambda_c)^2(a/c) \sin^{\frac{1}{2}}\theta. \quad (6)$$

This may be rewritten introducing τ_1 as

$$\tau = 0.56\tau_1(a/a_0) \sin^{\frac{1}{2}}\theta, \quad (7)$$

where a_0 is the Bohr radius.

Formula (6) or (7) well reproduces the whole experimental results, together with formula (3).

The analogy we have pointed out and developed here led us to deepen this study. A very detailed measurement of the angular distribution of the scattered light could show a complex behavior as is the case of electron-atom collisions.

Applications of this work may be found, for in-

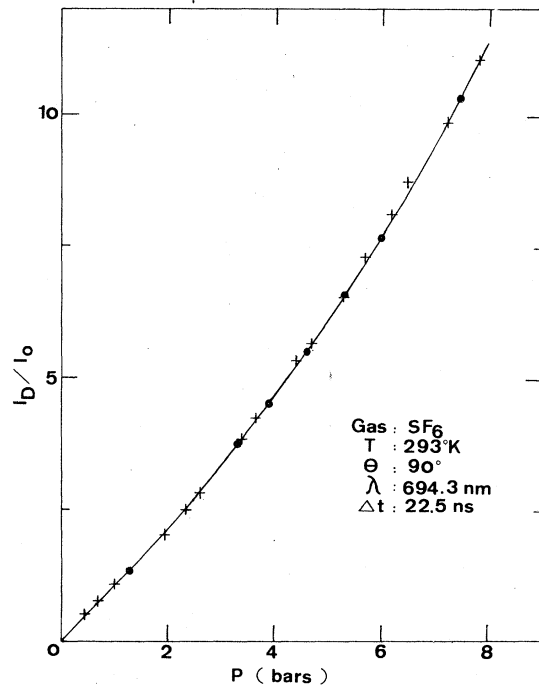


FIG. 10. Scattered light intensity I_D relative to the incident light I_0 in function of the pressure in SF₆. Black dots are experimental values obtained by Cazabat and Larour (Ref. 27). Crosses are the values obtained in our experiment. Full line is the state equation calculated with the Morsy (Ref. 28) formula.

stance, in the diagnostics of plasmas and in the transmission of short pulses of light through optical fibers (where the absorption is mainly due to the Rayleigh scattering).

ACKNOWLEDGMENTS

We acknowledge fruitful discussions with Professor L. Golstein and Professor Hans. R. Griem. We thank A. Leycuras and J. Lancelle for careful reading of the manuscript. We are grateful to J. Larour for fruitful discussions.

APPENDIX

Sulphur hexafluoride SF₆ has been studied in the pressure range from 1 to 10 atm. The scattered intensity is measured versus the pressure. We must now choose an equation of state for SF₆. Because it is far from a perfect gas, we may consider a Van der Waals model. As the deviation is 1% at low pressures and becomes 30% at 10 atm, it is then necessary to use a more accurate equation of state to describe the variation of the scattered light with pressure at constant temperature (293 K).

We use, following Cazabat and Larour²⁷ an empirical equation given by Morsy.²⁸

$$P = RTd + (B_0RT - A_0 - C_0/T^2)d^2 + (bRT - a)d^3 + (c/T^2)(1 + \gamma d^2)e^{-\gamma d^2}d^3 + a\alpha d^6, \quad (8)$$

where P is the pressure, R is the ideal gas constant, d is the molecular density, and A_0 , B_0 , C_0 , a , b , c , α , and γ are constants.

The experimental variation of the scattered intensity with the pressure is compared to the variation of the molecular density given by formula (8).

This comparison is displayed in Fig. 10. We have also given on this curve the experimental results obtained by Cazabat and Larour.²⁷ We are then able to determine precisely the scattered intensity at 1 atm and we calculate τ which in this case is 36 nsec.

*On leave from the Centre National de la Recherche Scientifique of Lebanon.

¹J. Cabannes, *La Diffusion Moléculaire de la Lumière* (Presses Universitaires de France, Paris, 1929).

²I. L. Fabelinskii, *Molecular Scattering of Light* (Plenum, New York, 1968).

³P. A. Fleury and J. P. Boon, *Laser Light Scattering in Fluid Systems, Advances in Chemical Physics* (Wiley-Interscience, New York, 1973), Vol. XXIV.

⁴P. Daure, C. R. Acad. Sci. **180**, 2032 (1925).

⁵J. Dufay and T. Kui, J. Phys. Radium **7**, 198 (1936); **1**, 251 (1940).

⁶J. Duclaux, J. Phys. Radium **6**, 401 (1935); **10**, 367 (1939).

⁷G. de Vaucouleurs, Ann. Phys. (Paris) **6**, 213 (1951).

⁸J. P. Geindre, J. C. Gauthier, and J. P. Delpech, Phys. Lett. A **44**, 149 (1973).

⁹T. V. George, L. Glodstein, L. Slama, and M. Yokokama, Phys. Rev. **137**, 369 (1965).

¹⁰R. D. Watson and M. K. Clark, Phys. Rev. Lett. **14**, 1057 (1965).

¹¹R. R. Rudder and D. R. Bach, J. Opt. Soc. Am. **58**, 1260 (1968).

¹²O. Theimer, Phys. Rev. Lett. **13**, 622 (1964).

¹³F. D. Feiock, Phys. Rev. **169**, 165 (1968).

¹⁴B. A. Sotskii, Opt. Spectrosc. (USSR) **24**, 526 (1968).

¹⁵G. J. Gabriel, Phys. Rev. A **8**, 963 (1973).

¹⁶J. Irisawa and P. K. John, Rev. Sci. Instrum. **44**, 1021 (1973).

¹⁷H. Ringler and R. A. Nodwell, Phys. Lett. A **29**, 151 (1969).

¹⁸C. R. Neufeld, Phys. Lett. A **31**, 19 (1970).

¹⁹S. R. Kimberlin, P. W. Chan, R. C. Hazelton, and E. J. Yablowski, J. Appl. Phys. **49**, 2700 (1978).

²⁰M. Skowronek, Y. Vitel, and C. Bayer, J. Phys. (Paris) **34**, 229 (1973).

²¹J. D. Kilkenny and M. S. White, Phys. Lett. A **55**, 209 (1975).

²²K. P. Selter and H. J. Kunze, Phys. Lett. A **68**, 57 (1978).

²³M. Skowronek, Y. Vitel, Y. Alayli, and C. Bayer, Phys. Lett. A **51**, 107 (1975).

²⁴Y. Alayli and M. Skowronek, in *Symposium on Physics of Ionized Gases, Dubrovnik, 1976*, edited by B. Navinsek (J. Stefan Institute, University of Ljubljana, Yugoslavia, 1977), p. 379.

²⁵N. J. Bridge and A. D. Buckingham, Proc. R. Soc. A **295**, 334 (1966).

²⁶I. Prigogine, in *Transfert d'Energie dans les Gaz 12th Conseil de Chimie* (Interscience, New York, 1962), p. 481.

²⁷A. M. Cazabat and J. Larour, J. Phys. (Paris) **36**, 1209 (1975).

²⁸T. E. Morsy, J. Chem. Eng. Data **15**, 256 (1970).